Cellular Physiology and Biochemistry

Cell Physiol Biochem 2013;32:1460-1472
DOI: 10.1159/000356583
Published online: November 28, 2013
Accepted: November 15, 2013

1421-9778/13/0325-1460$38.00/0

Original Paper

Molecular and Metabolic Consequences Following E6 Transfection in an Isogenic Ovarian Cell Line (A2780) Pair

Yuen-Li Chung[a,c] Eszter Nagy[b,c] Dominik Zietkowski[a] Geoffrey S. Payne[a]
David H. Phillips[b] Nandita M. deSouza[a]

[a]CR-UK and EPSRC Cancer Imaging Centre, The Institute of Cancer Research, Sutton, [b]Analytical and Environmental Sciences Division, King's College London, London, United Kingdom, [c]Authors contributed equally

Key Words
HPV E6 • Proton magnetic resonance spectroscopy • Glycerophosphocholine • Glutamine metabolism • Glucose metabolism • cPLA2 • Metabolomics

Abstract
Aims: To examine molecular and metabolic consequences of HPV-16 viral- protein E6, which targets p53 for degradation, in A2780 (ovarian cancer) cells. ***Methods:*** Isogenic derivatives of A2780 cells, with empty-vector (E6-) or E6 (E6+) transfection, were cultured. Intracellular metabolites, fatty acids, and the flux of glutamine, glucose, alanine and lactate in proliferation (Day 2) and confluence (Day 4) were determined using MRS. Western blotting confirmed p53 status, protein expressions related to AKT, ERK and mTOR signalling, and phospholipid metabolism. ***Results:*** Growth rate was slower in E6+ cells compared with E6-, resulting in reduced glycolysis, amino acid uptake and fatty acid synthesis. Glutamine metabolism, glycerophosphocholine (GPC), and protein expressions of cytosolic PLA2 (cPLA2) and p-cPLA2 increased in E6+ cells. Despite decreased ERK and AKT signalling, expression of S6RP and p-S6RP downstream of mTOR remained unaffected in E6+ cells. E6+ cells were more invasive and migrate faster than the E6- cells. ***Conclusion****:* E6+ had slower growth than E6- cells with reduced metabolism, but E6+ cells maintained cellular homeostasis through glutamine metabolism when compared with E6- at Day 2. The ability to migrate and form larger colonies may provide the E6+ cells with a growth advantage.

Dr. Y-L Chung
CR-UK and EPSRC Cancer Imaging Centre, The Institute of Cancer Research and Royal Marsden NHS Foundation Trust, Sutton, Surrey SM2 5NG, (United Kingdom)
Tel. +44-20-8661 3245, Fax +44-20-8661 0846, E-Mail ylichung@icr.ac.uk

Introduction

Four out of five women will acquire human papilloma virus (HPV) infection at some point in their lives. Of the 100 types of HPVs identified, approximately 30 to 40 infect genital tract mucosa and are categorized as either low- or high-risk, the former being associated primarily with benign genital warts, whereas the latter are associated with anogenital cancers, especially cervical cancer [1]. The ability of HPV infections to cause cancer has been attributed to the actions of the E6 and E7 proteins and their ability to manipulate cell cycle regulators such as p53 [2]. Binding of the E6 protein to a cellular ubiquitin-ligase, the E6-associated protein (E6-AP), which in turn binds the p53 protein [3] initiates p53 proteolysis by the proteasome [4] through the ubiquitin complex of enzymes. The degradation of p53 results in bypassing of growth arrest signals at the G1/S and G2/M checkpoints, which results in the instigation of malignant transformation [2]. More recently p53 has been found to be a key regulator of many important metabolic pathways to maintain metabolic homeostasis and reported to play a role in glucose metabolism, mitochondrial respiration, glutaminolysis and regulation of cell growth via interaction with the mTOR pathway [5].

In cervical cancer tissue, where the presence of HPV is common, magnetic resonance spectroscopy (MRS) studies have demonstrated increased choline-containing compounds and creatine, including a characteristic, intense methylene resonance at 1.3 ppm, compared with non-cancer cervical tissue [6, 7]. Mobile lipid resonances (MLR) at 0.9 ppm and 2.0ppm are also increased in cervical cancer compared to pre-invasive (CIN) tissue [8, 9]. However, because of the prevalence of HPV infection in these patients, the metabolite patterns specifically associated with the effects of viral proteins cannot be distinguished in these tissue studies. Therefore, although it is expected that cells transfected with HPV E6 will have reduced p53 expression and a subsequent increase of glycolysis [5, 10, 11] and activation of signalling pathways to support increased growth rate with corresponding changes in metabolism, the metabolic effects of HPV infection and subsequent p53 proteolysis are poorly documented in cervical cancer. No studies documenting differences in the spectral patterns between E6+ and E6- tissues have yet been described. Previous studies have shown the ovarian cell line A2780 to be a suitable model for the functional changes observed due to HPV infection, and to study the impact of E6 expression in cancer and cancer treatment [12-15]. Therefore the purpose of this study was to examine the molecular and metabolic consequences following transfection with the HPV-16 E6 protein in A2780 ovarian cancer cells.

Material and Methods

Chemicals

All chemicals used were of analytical grade where applicable and purchased at the following sources: Dulbecco's Modified Eagle Medium (D-MEM, low and high glucose), Foetal Bovine Serum (FBS, Heat-Inactivated) 100 X MEM non-essential amino acids (NEAA), NuPAGE® 4-12% Bis-Tris Gels, MES Running Buffer, Transfer Buffer, 0.2µm nitrocellulose membrane and propidium iodide (1.0 mg/ml) all from Invitrogen (now Life Technologies), Carlsbad, USA; RNase A (100 mg/ml) from Qiagen Gmbh, Hilden, Germany; Puromycin dihydrochloride (*Streptomyces alboniger*) and Crystal Violet powder, both from Sigma-Aldrich Gmbh, Steinheim, Germany; Bicinchoninic Acid (BCA) protein assay kit and SuperSignal® West Pico Chemiluminescent Substrate from Thermo Scientific, Rockford, USA; Anti-p53 (Ab-6, Pantropic) Mouse mAb from Calbiochem, Merck Nottingham, UK; Anti-mouse HRP-conjugate antibody from Biorad, Hertfordshire, UK.

Cell culture

Human, ovarian cell lines kindly provided by Dr Michael I. Walton from the Institute of Cancer Research were used. Isogenic cell line pairs were established by transfecting A2780 with either an empty vector expressing puromycin resistance alone (plasmid F179) or a vector expressing HPV-16 E6 protein and

puromycin resistance (plasmid F192). The success of the transfection process was assessed through p53 expression [15]. Both isogenic lines, *E6-* (empty-vector control) and *E6+* (E6 transfected), were cultured in D-MEM containing 10% FBS in 5% CO_2 and at 37°C. Construct expressing cells were selected for by using 2 μg/mL of puromycin for three days, after which the puromycin was removed and cells were given fresh culture media and left for 48 hours to recover. For cell extract experiments, cells were trypsinized, diluted with culture media to a total volume of 15 mL and portioned into 1-mL aliquots for cell cycle analysis (FACS) for western blotting, a 2-mL aliquot for cell viability, and the rest used for extraction and MRS analysis.

Growth Curves

Doubling times and cell sizes were measured in E6- and E6+ cell lines at log (Day 2) and confluent (Day 4) phases. These selected time-points reflected previous growth curve analysis which showed that at 2 days post-seeding the cells were in the log phase of growth, whereas at 4 days they reached the confluence. To establish the growth curves, the isogenic lines were seeded in T25 flasks with a density of 300,000 cells per flask and harvested every day for five days with three flasks at each time point. Cells were trypsinized for 2 min at 37°C, diluted in 2.5 mL of culture media and counted on an automated system (Vi-Cell Cell Viability Analyser, Beckman Coulter Inc, High Wycombe, UK). Once the log-phase was established, 2 million cells from each line were seeded in T175 flasks and harvested at log phase and at confluence.

Cell cycle analysis with flow cytometry

In order to investigate the effect of E6 transfection on cell cycle, we performed fluorescence-activated cell sorting (FACS analysis) on E6- and E6+ A2780 cells at Day 2 and 4. Harvested cells were washed 2 x 1 mL in cold PBS and centrifuged at 2000 rpm for 4 min at 4 ºC. Cell pellets were resuspended in 100 μL cold PBS and diluted to 2 mL with 70% of cold ethanol and stored at -20 °C until analysis. Cells were centrifuged at 2000 rpm for 4 min at 4 °C, supernatant removed and pellet resuspended in 1 mL of PBS containing 100 μg/mL RNase A and 40 μg/mL propidium iodide. Cells were incubated for 30 min at 37°C and stored at 4 °C until analysis on a BD LSR II flow cytometer with accompanying BD FACS DiVa software (version 6.1.3, from BD Biosciences, Oxford, UK). Data were collected from 10,000 counts per sample.

Dual Phase Extraction of cells

In order to examine the metabolic consequences following the down-regulation of p53 by E6 protein, examinations of metabolic profiles on E6- and E6+ A2780 cells were performed in the log phase (exponential growth, Day 2), as well as the confluent state (Day 4) of the cells, as determined by the growth curves. Cells were harvested and extracted by dual phase extraction procedures as previously described at these time points [16].

^{1}H-MRS of cell extracts and culture media

Water-soluble extracts were freeze-dried and reconstituted in 580 μL deuterated water (D_2O, Sigma Aldrich) and 20 μL of 0.75% sodium 3-trimethylsilyl-2,2,3,3-tetradeuteropropionate (TSP) in D_2O (Sigma Aldrich) was added to the samples for chemical shift calibration and quantification [16]. 500 μL of the extract solution was then placed in 5 mm NMR tubes and samples were pH to 9. Lipid extracts were reconstituted in 450 μL deuterated chloroform (Sigma Aldrich) and 150 μL of 0.1% tetramethylsilane in deuterated chloroform (Sigma Aldrich) was added to the samples for chemical shift calibration and quantification. Culture media samples from the E6- and E6+ cells line at Day 2 and 4 were collected before cells were harvested for cellular extractions. 500 μL of media sample and 50 μL of D_2O were placed in the NMR tube, and 50 μL of 0.75% TSP in D_2O was added to the samples for chemical shift calibration and quantification. Spectral assignments were based on literature values [17, 18].

^{1}H-MRS was performed using a Bruker 500MHz spectrometer (Bruker Biospin, Coventry, UK) and spectra were acquired with 7500Hz spectral width, 16K time domain points, relaxation delay 2.7s, 256 scans, temperature 298K. Spectral processing was carried out using the Bruker Topspin-2 software package (Bruker Biospin, Coventry, UK). Metabolite levels are standardised to cell number and volume.

Western blot analysis

In order to investigate the mechanism that drives the growth characteristic and cellular metabolism in the E6 transfected cells, we used western blots to examine the expression of various proteins in the c-MYC,

AKT, ERK and mTOR signalling pathways and in the phospholipid metabolism pathways. E6- and E6+ cells were harvested at Day 2 and 4 and cells centrifuged at 2000 rpm for 4 min at 4 ºC. Medium was removed and cells were washed in 2 x 1 ml PBS and centrifuged as above. The cell pellet was dissolved in 200 µL lysis buffer (62.5mM Tris-HCl, pH 7.4, 2% SDS, 10% Glycerol and 1mM EDTA). Protein concentration was determined using the BCA assay, followed by normalization and denaturation with ß-mercaptoethanol at 80 °C for 15 min. Samples (15 µg) were then loaded onto 4-12% Bis-Tris gels and separated at 130V, subsequently transferred onto a nitrocellulose membrane at 30V for 2 h, respectively. The membrane was blocked in 5% w/v non-fat milk dissolved in 0.2% TBS-T (Tris Buffered Saline containing 0.2% Tween-20), then probed overnight at 4°C for FASN (#3189, 1:100), cPLA (#2832, 1:1000), p-cPLA (#2831, 1:1000), c-MYC (#9402, 1:500), p-AKT (#2965, 1:1000), AKT (#9272, 1:4000), ERK (#4695, 1:1000), p-ERK (#4370, 1:1000), S6RP (#2217, 1:1000), and p-S6RP (#2215, 1:1000; all ten from Cell Signalling), as well as MCT-1 (#sc-14916, 1:1000) and LDH-A (#sc-27230 1:1000; both from Santa Cruz Biotechnology) in 5% w/v BSA in 0.2% TBS-T. Additionally, p53 (#OP43, 1:2000 from Calbiochem) and loading control GAPDH (#MAB374 1:10000 from Millipore) were used in 3% milk at RT for one hour. Following secondary anti-mouse (#170-5047, 1:10000), anti-rabbit (170-5046, 1:10000) and anti-goat (#172-1034, 1:10000, all three from Bio-Rad) incubation for 1h at RT, the membrane was visualized through chemiluminescence (SuperSignal West Pico, Thermo Scientific).

Colony formation in agarose

2 X D-MEM (high glucose) was supplemented with 20% FBS, 20% penicillin-streptomycin and 2 X non-essential amino acids. Low melting point agarose was dissolved in sterile PBS in 1.5% and 0.9% solutions and then placed in a water bath to cool down to 37 °C. The 2 X D-MEM and 1.5% agarose were mixed 1:1 and 2mL of the mix was plated in each well in a 6-well plate. When solidified, an upper layer of 0.9% agarose was mixed with 2X D-MEM (1:1) containing either E6- or E6+ cells and plated into the wells in 2 mL volume corresponding to 3000 cells/well. Once the upper layer solidified, the embedded cells were moved into an incubator. Once a week, 200 µL of 1 X D-MEM was added to the cells in order to prevent gels from drying. Cells were left to grow for three weeks, after which they were fixed with 500 µL of 10% methanol and 10% acetic acid in water. After 30 min the solution was removed and colonies were stained for one hour with 0.05% crystal violet in 10% methanol. Experiments were done in triplicate.

Migration Assay

Cell lines were seeded in a 6-well plate each and were allowed to grow in parallel in regular growth media D-MEM until reaching confluence. The growth medium was then removed, cells were washed twice with PBS and with a sterile pipette tip a line was carefully drawn across the bed of cells, removing them in a path. Great care was taken not to damage the plastic surface, which would prevent cells from attaching during migration. New medium was added to the cells, which were continuously monitored from then on. Images were taken from the time of "scratching" up to 72 hours, when one of the cell lines covered the barren area anew.

Statistical Analysis

Data are expressed as mean ± SD. For comparison of metabolic flux, metabolite concentrations and ratios, unpaired Student's standard t-tests were used and Bonferroni corrections were applied. All statistical tests were two-sided.

Results

Growth curve and cell size

The doubling time of E6+ A2780 cells was similar to E6- A2780 cells on day 2 (~24 hours), but it became about 11% longer in E6+ A2780 cells (~22 hours) than *E6-* A2780 cells (~19.5 h; $p<0.007$), leading to approximately 32% lower cell densities in E6+ cells on day 4 of the culture (Day 2, *E6+* $8.0\pm1.0\times10^6$ cells, *E6-* $8.7\pm1.0\times10^6$ cells; Day 4, *E6+* $35.7\pm2.9\times10^6$ cells, *E6-* $52.6\pm1.0\times10^6$ cells) (Fig. 1A). E6+ cells were on average 1.0 µm larger in diameter (12.9±0.2µm) compared to the E6- cells (11.9±0.3 µm) on day 2 but the E6+ cell size

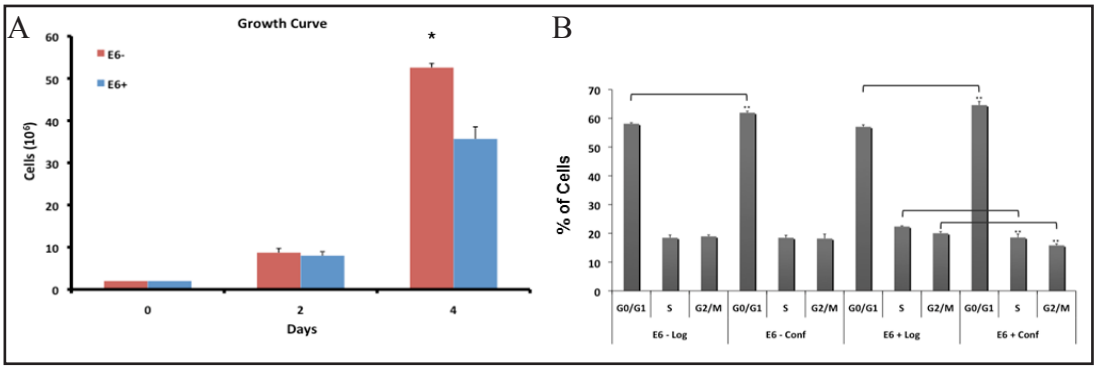

Fig. 1. (A) Growth curve of A2780 E6- and E6+ cells. *p<0.01. (B) FACS analysis of the cell cycle of E6- and E6+ cells in log phase of growth and at confluence (n=4 for each cell line). There was a significant increase in the proportion of E6+ cells in G_1 (p=0.004), and significantly decreased in both S- (p=0.009) and G_2/M-phase cells (p=0.003) on Day 4 compared with Day 2. In E6- cells, a small, but significant increase in G_1 phase (p=0.002) was observed on Day 4 when compared with Day 2. ** p < 0.01.

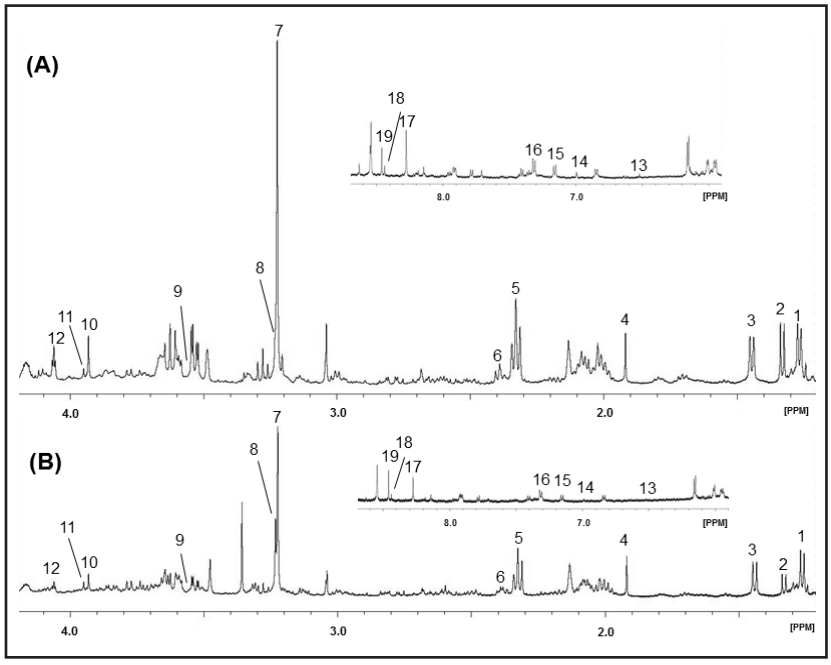

Fig. 2. Representative 1H MRS spectra of water-soluble metabolites in cell extracts of (A) E6- and (B) E6+ at Day 2. Spectral assignments: (1) threonine; (2) lactate; (3) alanine; (4) acetate; (5) glutamate; (6) glutamine; (7) phosphocholine; (8) glycerophosphocholine; (9) glycine; (10) creatine; (11) phosphocreatine; (12) myo-inositol; (13) fumarate; (14) histidine; (15) tyrosine; (16) phenylalanine; (17) ATP and ADP; (18) NAD(H); (19) formate.

decreased on day 4 (11.9±0.2 μm), while the size of E6- cells remained unchanged on Day 4. The viability of the E6+ cells, at Day 2 and 4 was comparable, 95.9±2.8% and 92.4±1.6%, respectively, as was the viability of E6- cells (93.9±2.4% on Day 2 and 90.8±1.1% on day 4). Additional differences between the cell lines were the extent of adhesion, where E6+ formed a strongly attached monolayer along the surface, whereas E6- accumulated in clusters that easily detached from the flask.

Cell cycle analysis by flow cytometery

There was a significant increase in the proportion of E6+ cells in G_1 (p=0.004), and significantly decreased in both S- (p=0.009) and G_2/M-phase cells (p=0.003) on Day 4 compared with Day 2 (Fig. 1B). In E6- cells, a small, but significant increase in G_1 phase (p=0.002) was observed on Day 4 when compared with Day 2 (Fig. 1B). There were no significant changes observed in S- or G_2/M-phase cell distributions. E6+ cells showed significant increases in the S phase (p=0.0002) and G_0/G_1 phase (p=0.009) at Day 2 and 4, respectively, when compared with E6- cells.

Metabolite Concentration	Day 2 E6- Mean ± SD (fmol/1000μm³ cell)	Day 2 E6+ Mean ± SD (fmol/1000μm³ cell)	p	Day 4 E6- Mean ± SD (fmol/1000μm³ cell)	Day 4 E6+ Mean ± SD (fmol/1000μm³ cell)	p
Threonine	0.39 ± 0.02	0.23 ± 0.03	<0.0001	0.22 ± 0.01⁺	0.23 ± 0.05	NS
Lactate	0.42 ± 0.02	0.13 ± 0.04	<0.0001	1.12 ± 0.08⁺	0.36 ± 0.12	<0.0001
Alanine	0.43 ± 0.05	0.16 ± 0.02	<0.0001	0.60 ± 0.03⁺	0.49 ± 0.09*	NS
Glutamate	0.94 ± 0.03	0.46 ± 0.05	<0.0001	0.70 ± 0.04⁺	0.62 ± 0.13	NS
Glutamine	0.22 ± 0.02	0.11 ± 0.02	0.0002	0.28 ± 0.02	0.25 ± 0.04*	NS
Phosphocholine	0.33 ± 0.01	0.14 ± 0.01	<0.0001	0.15 ± 0.01⁺	0.18 ± 0.03	NS
GPC	0.03 ± 0.01	0.06 ± 0.01	0.0002	0.007 ± 0.002⁺	0.03 ± 0.01*	0.0005
Glycine	0.014 ± 0.002	0.005 ± 0.001	0.0005	0.01 ± 0.01	0.02 ± 0.01*	NS
Creatine	0.13 ± 0.01	0.05 ± 0.01	<0.0001	0.08 ± 0.01⁺	0.08 ± 0.01	NS
phosphocreatine	0.03 ± 0.01	0.02 ± 0.01	NS	0.04 ± 0.01	0.08 ± 0.03	NS
Myo-inositol	0.22 ± 0.02	0.06 ± 0.01	<0.0001	0.14 ± 0.06	0.11 ± 0.02	NS
Fumarate	0.003 ± 0.001	Not detected	0.0004	0.004 ± 0.001	0.004 ± 0.01*	NS
Histidine	0.019 ± 0.008	0.005 ± 0.005	NS	0.016 ± 0.001	0.013 ± 0.002	NS
Tyrosine	0.037 ± 0.004	0.023 ± 0.002	NS	0.041 ± 0.002	0.023 ± 0.004	0.0002
Phenylalanine	0.062 ± 0.003	0.048 ± 0.006	NS	0.047 ± 0.004	0.031 ± 0.003	0.0004
ATP + ADP	0.12 ± 0.02	0.05 ± 0.01	0.001	0.09 ± 0.02	0.07 ± 0.01	NS
NADH + NAD	0.014 ± 0.003	0.013 ± 0.003	NS	0.018 ± 0.002	0.017 ± 0.003	NS

Table 1. Water-soluble metabolites in E6- and E6+ cells at day 2 and 4. Significant differences between E6- and E6+ at day 2 and 4 are shown. ⁺ indicate significant differences between Day 2 and Day 4 in E6- cells. * indicate significant changes between Day 2 and Day 4 in E6+ cells. Data are Bonferroni corrected. GPC – glycerophosphocholine

Metabolomic study of E6+ and E6- A2780 cells

^{1}H-MRS spectra of water-soluble metabolites in cell extracts of E6- and E6+ at Day 2 are shown in Fig. 2. The quantified levels of low molecular weight water-soluble and lipid metabolites at Day 2 and 4 from cell extracts of the E6- and E6+ cells are shown in Tables 1 and 2 respectively.

Longitudinal assessment of cellular metabolites in each cell line

A longitudinal comparison in the E6+ cells showed increases in cellular alanine (p=0.0005), glutamine (p=0.0005), glycine (p=0.003), fumarate (p=0.0003), phosphatidylcholine (p=0.001), saturated (p=0.002) and unsaturated fatty acids (p=0.001) and a decrease in glycerophosphocholine (GPC, p=0.001) on Day 4 when compared with Day 2 (Table 1 and 2), suggesting continued proliferation in these cells. In contrast, the E6- cells showed significant increases in cellular threonine (p<0.0001), lactate (p<0.0001) and alanine (p=0.002), and decreases in glutamate (p<0.0001), phosphocholine (p<0.0001), GPC (p<0.0001), creatine (p=0.0002) and unsaturated fatty acids (p<0.0006) at Day 4 when compared with Day 2 (Table 1 and 2), indicating a slowing of their metabolism as they reached confluence.

Comparison of cellular metabolism and anaerobic glycolysis in E6+ vs. E6-cells at Day 2

At Day 2, cellular water-soluble metabolites (threonine (p<0.0001), glutamine (p=0.0002), glutamate (p<0.0001), fumarate (p=0.0004), glycine (p=0.0005), phosphocholine

Lipid/$CDCl_3$ ratio	Day 2 *E6-* Mean ± SD (/million of 1000μm³ cells)	Day 2 *E6+* Mean ± SD (/million of 1000μm³ cells)	Day 2 p	Day 4 *E6-* Mean ± SD (/million of 1000μm³ cells)	Day 4 *E6+* Mean ± SD (/million of 1000μm³ cells)	Day 4 p
CH3 FA	0.103 ± 0.016	0.048 ± 0.002	0.0004	0.065 ± 0.005	0.072 ± 0.012	NS
(CH2)n FA	0.74 ± 0.12	0.33 ± 0.02	0.0006	0.49 ± 0.05	0.55 ± 0.08*	NS
-CH2-CH2-CH=	0.085 ± 0.012	0.038 ± 0.003	0.0003	0.061 ± 0.006	0.069 ± 0.001*	NS
-O2C-CH2-CH2-	0.065 ± 0.010	0.028 ± 0.002	0.0004	0.047 ± 0.005	0.053 ± 0.007*	NS
=CH-CH2-CH=	0.027 ± 0.004	0.011 ± 0.001	0.0002	0.014 ± 0.002+	0.014 ± 0.003	NS
-CH2=CH2-	0.055 ± 0.007	0.024 ± 0.002	0.0001	0.038 ± 0.003	0.041 ± 0.006*	NS
PtdE	0.004 ± 0.001	0.002 ± 0.001	NS	0.002 ± 0.001	0.003 ± 0.001	NS
PtdC	0.062 ± 0.009	0.024 ± 0.003	0.0003	0.058 ± 0.007	0.056 ± 0.010*	NS
Triacylglycerol	0.003 ± 0.001	0.002 ± 0.001	NS	0.004 ± 0.001	0.004 ± 0.001	NS
Plasmogen	0.001 ± 0.001	0.001 ± 0.001	NS	0.001 ± 0.001	0.001 ± 0.001	NS

Table 2. Lipid metabolites in E6- and E6+ cells at day 2 and 4. Significant differences between E6- and E6+ at day 2 and 4 are shown. + indicate significant differences between Day 2 and Day 4 in E6- cells. * indicate significant changes between Day 2 and Day 4 in E6+ cells. Data are Bonferroni corrected. PtdE – phosphatidylethanolamine, PtdC – phosphatidylcholine

(p<0.0001), GPC (p=0.0002), creatine (p<0.0001), myo-inositol (p<0.0001) and ATP+ADP (p=0.001), phosphatidylcholine (p=0.0003)) and lipid metabolites (saturated (p<0.0006) and unsaturated (p<0.0005) fatty acids) were 2 to 3 fold lower in the E6+ when compared with E6- cells (Table 1 and 2). This was accompanied by significantly lower uptakes of leucine (p<0.0001), valine (p=0.0004), iso-leucine (p=0.0004), glutamine (p<0.0001), histidine (p=0.0007), tyrosine (p<0.0001) and phenylalanine (p<0.0001) from culture medium in E6+ compared to E6- cells (Fig. 3). The lower cellular metabolism is consistent with slower cell growth and proliferation in E6+ compared to E6- cells during the log phase of growth. At this time point E6+ cells also showed significantly lower cellular lactate (p<0.0001) and alanine (p<0.0001), glucose uptake (p<0.0001) and lactate excretion (p<0.0001) in the culture media compared with E6- cells indicating that E6-transfection in A2780 cells reduces glucose metabolism and Warburg effect during the log phase of growth.

Comparison of cellular metabolism and glycolysis in E6+ vs. E6- cells at day 4

At Day 4, higher cellular GPC (p=0.0005) and lower cellular lactate (p<0.0001), tyrosine (p=0.0002) and phenylalanine (p=0.0004) were observed in *E6+* cells when compared to *E6-* cells, while other cellular metabolites were not significantly different between the two cell lines (Table 1). From the measurements of the culture medium, uptake of glucose (p<0.0001), leucine (p<0.0001), valine (p=0.0002), iso-leucine (p=0.0001), glutamine (p<0.0001), histidine (p<0.0001), tyrosine (p<0.0001), phenylalanine (p<0.0001) was significantly greater and lactate (p=0.0002) and alanine (p<0.0001) excretion was higher in E6+ cells compared with E6- cells at Day 4 (Fig. 3). No difference in cellular lipids was observed between the two cell lines (Table 2). This indicates higher cellular metabolism in E6+ than E6- cells at Day 4, likely due to the continued proliferation of E6+ cells whereas cellular metabolism slowed in E6- cells as they reached confluence.

Protein expression analysis

To investigate the mechanisms responsible for the observed metabolic changes, we examined the c-MYC and PI3K/mTOR pathways, as well as expression of LDH-A, MCT-1, cPLA2, p-cPLA2, and FASN. In addition, *E6-* cells constitutively expressed p53, whereas it was absent in the *E6+* cells at both Day 2 and 4, confirming reduced level of p53 by the presence of E6 protein (Fig. 4). Western blots for the expressions of p53, c-MYC, AKT, p-AKT, ERK, p-ERK, S6RP, pS6RP, LDH-A, MCT-1, cPLA2, p-cPLA2, and FASN in E6+ and E6- cells at Day 2 and 4 are illustrated in Fig. 4.

Assessment of mTOR c-MYC, AKT and ERK pathways

Expression of c-MYC, p-AKT, ERK and p-ERK was lower in the E6+ cells at Day 2 and 4 when compared with E6- cells at Day 2, indicating down-regulation of c-MYC, AKT and ERK pathways in the E6+ cells with no differences observed in the pS6RP and S6RP expression. This indicates that the downstream mTOR pathway is unaffected (Fig. 4), and suggesting that mTOR activation in the E6+ cells is independent of the AKT and ERK pathways.

Decreased levels of p-AKT, p-ERK and p-S6RP in the E6- cells at Day 4 compared with Day 2, were consistent with the AKT, ERK and mTOR pathways being down-regulated as proliferation reduced and cells reached confluence.

Anaerobic glycolytic enzyme expression

The expression of LDH-A was lower in E6+ cells at both time-points when compared with the control (Fig. 4). This was consistent with the down-regulated c-MYC, AKT and ERK pathways. The monocarboxylate transporter-1 (MCT-1) expression was lower in the E6+ cells at Day 2 but increased to control levels by Day 4 (Fig. 4), consistent with reduced lactate excretion at Day 2 and enhanced excretion at day 4 in E6+ compared with E6- cells. These findings together with the metabolomic data indicate that the E6+ A2780 cells, with decreased level of p53, have a reduced glucose metabolism and Warburg effect at Day 2 compared with the E6- cells, but that these metabolic effects increase at Day 4.

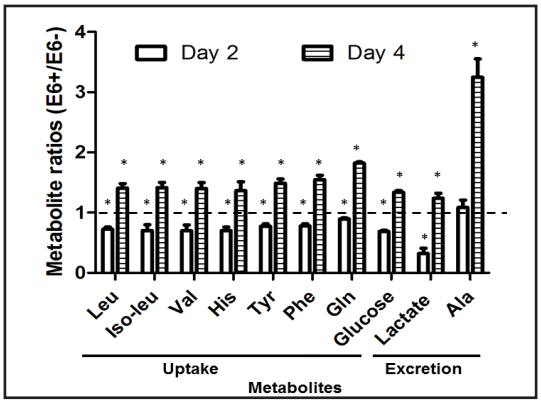

Fig. 3. Metabolite uptake and excretion in the media of E6- and E6+ A2780 cells at Day 2 and 4. Keys-leucine (Leu); isoleucine (Iso-leu); valine (Val); histidine (His); tyrosine (Tyr); glutamine (Gln); alanine (Ala).

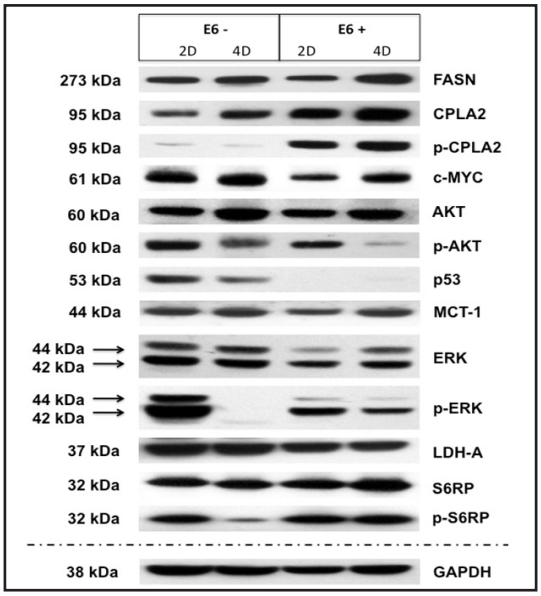

Fig. 4. Western blot analysis of FASN, cPLA2, p-cPLA2, c-MYC, AKT, p-AKT, p53, MCT-1, ERK, p-ERK, LDH-A, p-S6RP and S6RP expressions in the cell lysates of the E6- and E6+ A2780 isogenic cells collected at Day 2 and 4. GAPDH was used as a loading control.

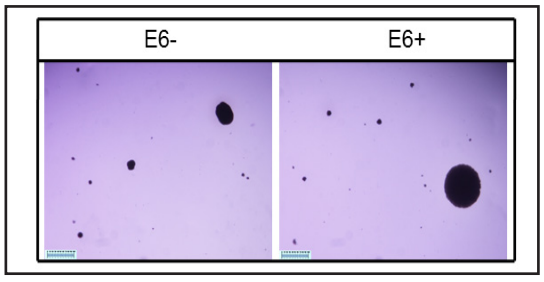

Fig. 5. Representative images of colony formation in agarose of E6- and E6+ cells with different size-range.

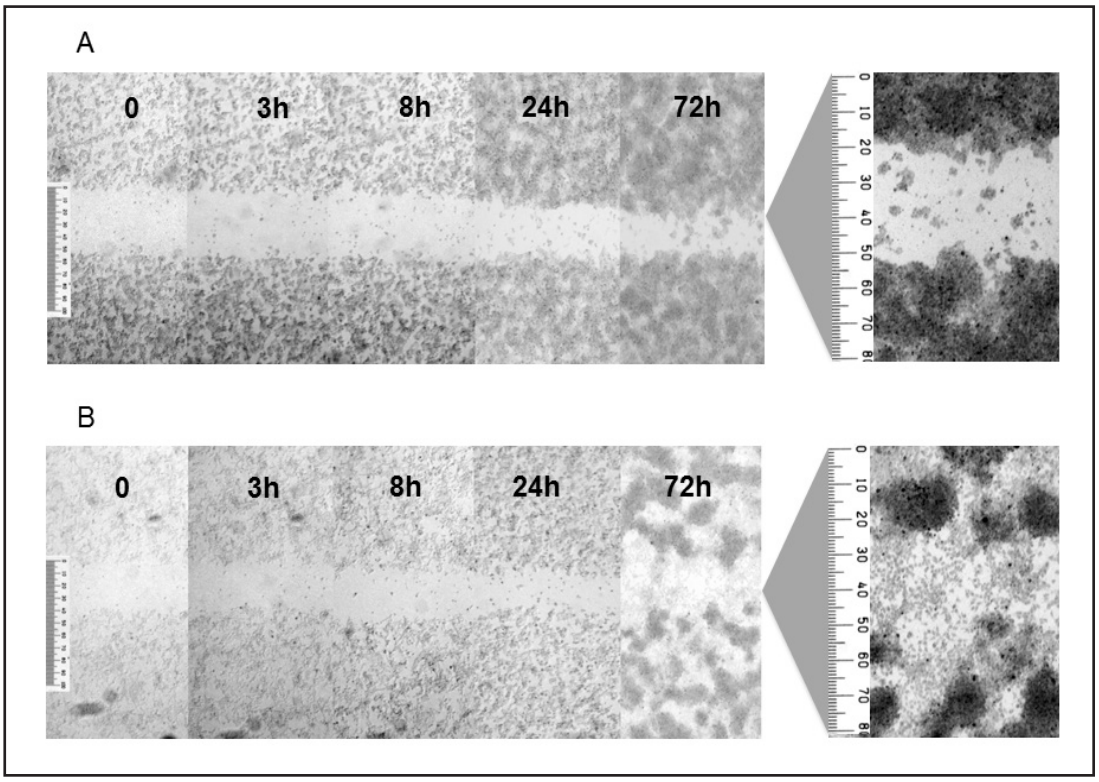

Fig. 6. Images of E6- (A) and E6+ (B) cells migrated through a 500μm and 400μm gap, respectively, at 0, 3, 8, 24 and 72 hours. The enlarged images showed the migration of E6- and E6+ cells at 72 hours.

Lipid metabolism

The decreased expression of fatty acid synthase (FASN) at Day 2 (which later increased at Day 4) in E6+ cells compared with E6- cells (Fig. 4), was consistent with the levels of saturated and unsaturated fatty acids observed at the two time points (Table 2). These differences even out over time and become equivalent to what was observed in E6- cells at Day 4, supporting the lower proliferation rates in the E6+ cells at Day 2 and the continued proliferation at Day 4 when compared with E6- cells.

Protein expression of total cPLA2 and p-cPLA2 in both isogenic lines and time points, was performed to investigate the reason for the persistently elevated levels of GPC in E6+ cells. The results confirmed a higher expression of total cPLA2 and p-cPLA2 at both time-points in E6+ cells (Fig. 4), supporting that GPC synthesis from phosphatidylcholine in E6+ cells is catalysed by cPLA2.

Colony formation

Colony formation (Fig. 5) in agarose over a period of three weeks, revealed no statistical difference between the two isogenic lines with 85 ± 16 and 71 ± 15 for E6+ and E6-, respectively. The colonies were defined as below 30 nm, between 30-70 nm and above 70 nm. Colonies above 70 nm were also similar in numbers with a total of seven in E6+ and five in E6- in all three cultures. However, the largest colonies, ranging between 100-180nm were found in E6+, whereas the largest colony in E6- was 120 nm.

Migration Assay

Both cell lines reached confluence at the same day and were "scratched" at the same time and monitored in parallel. Photographs were taken up to 72 hours post-scraping. Neither of the cell lines had the ability to migrate to the barren area within the first 24 hours (Fig. 6A and B) although they continued proliferating. The width of the line, which was 500

μm in the case of the E6- cells, was reduced to about 300 μm after 72 hours. Although small islands of clustered cells had attached along the path, the contrast to the thickness of the over-confluent surrounding suggests that virtually no, or very limited, re-growth has taken place (Fig. 6A).

The more adherent cells (E6+) started attaching to the clear area after 24 hours and by 72 hours the line was re-grown, although only as a monolayer. Due to being more adherent, the initial line width was 400 μm wide, compared to that of the E6- cells (Fig. 6B). Nonetheless, even the E6+ cells continued to cluster in "patches", not evenly as in the case of the E6- cells, before migrating to the barren area.

Discussion

Our data indicate that despite the down-regulation of p53, E6+ cells grow more slowly than the E6- cells at Day 2 and that this is accompanied by corresponding metabolic changes associated with slower growth. Lower cellular metabolites along with reduced amino acid and glucose uptake in E6+ cells compared to empty vector controls were seen during the log phase of growth and became comparable with levels in the controls only when the latter reached confluence. The decreases in growth rate and cellular metabolism in the p53 absent E6+ A2780 cells were therefore surprising and unexpected. E6 and E7 in HPV type 16 are reported to induce invasive and metastatic abilities of MCF7 and BT20 (non-invasive breast cancer cell lines) *in vitro* and *in vivo*, respectively, in comparison with the wild type cells [19]. E6 and E7 expressing cells also exhibit a significant metastatic activity compared with the parental population cell lines [19]. In a clinical study of cervical cancer, E6 variants were more prevalent in invasive cervical carcinoma, indicating that the E6 variants may be more oncogenic than other variants and thus carry a higher risk for the development of invasive cervical disease [20]. However, it may be that the effects on growth rate are dissociated from the effects on ability to invade and metastasize.

The reduced glucose metabolism and Warburg effect in the E6+ cells as evidenced by lower cellular lactate, lactate excretion and glucose uptake together with reduced LDH-A expression at Day 2 are surprising following the down-regulation of p53 expression. Previous studies have shown that the tumour suppressor p53 can reduce the glycolytic flux via various routes [5, 10], such as down-regulation of glucose transporter expressions [21], inhibition of NF-κB [11] and direct inhibition of glucose-6-phosphate dehydrogenase [22]. Despite lower intracellular lactate, more lactate was excreted from the E6+ cells into the culture media than the E6- cells on Day 4. This may be explained by the effects of the down-regulation of p53 increasing MCT-1 expression and enhancing lactate export [23].

mTOR signalling is a key pathway for protein synthesis and cell growth. This study indicates that proliferation in the E6+ cells was maintained by an up-regulated mTOR signalling pathway independent of the AKT and ERK pathways. This suggests that upstream signalling pathways other than the PI3K cascade may activate/control the mTOR signalling. Although outside the scope of this study, observations in the literature suggest a likely candidate to be the Wnt pathway. Previous reports have shown that the E6 protein can activate the Wnt pathway in the epidermis of transgenic mouse expressing full-length E6 oncoprotein [24], and in HPV16-positive oropharyngeal squamous carcinoma cells [25]. The activation of the Wnt signalling pathway and of mTOR signalling has also been observed in tumour samples from the E6 variants non-European cervical cancer patients [26].

Cellular homeostasis appeared to be maintained initially by glutamine metabolism rather than glycolysis in E6+ cells. This is indicated by the significantly lower lactate excretion (~33%), glucose uptake (~70%), and decreased levels of cellular glutamine and glutamate (~50%), compared with the E6- cells. In addition, although glutamine uptake was only 10% lower in the E6+ cells than in the E6- cells, the alanine excretion was quite similar (Fig. 3). This suggests that cellular homeostasis in the cells with reduced p53 level, may be sustained by glutamine metabolism rather than glycolysis at Day 2. When comparing the two cell lines

at Day 4, on the other hand, glucose and glutamine uptake increases in E6+ (134% and 182%, respectively) along with elevated excretion of lactate (124%) and alanine (325%), indicating a switch in cellular homeostasis maintained by both glutamine metabolism and glycolysis in E6+ cells at this time point. This is in line with previous reports showing that glutamine is used for biosynthesis and mitochondrial metabolism in cancer cells, whereas lactate, alanine and ammonia are produced following glutaminolysis [27-29].

GPC was higher in E6+ cells at both time points together with increased cPLA2 and p-cPLA2 expression. GPC is synthesised from phosphatidylcholine and cPLA2 is the first enzyme in this pathway. Cytosolic PLA2 was found to promote proliferation of vascular endothelial cells and formation of a functional tumour vascular network [30, 31]. Decreased cPLA2 has been shown to be associated with reduced proliferation and invasive migration in lung and brain cancer. It is required for pericyte recruitment and vessel maturation, thus plays an important regulatory role in tumour angiogenesis [32]. Reduction in GPC was also found in tumours following treatment with the vascular disruption agent, 5,6-dimethylxanthenone-4-acetic acid [33] and the HDAC inhibitor, LAQ824, that caused a decrease in microvessel density [34]. The consistently elevated levels of cPLA2, p-cPLA2 and GPC observed in the E6+ cells suggests that either reduced level of p53, or the influence of the viral-protein E6 may be involved in the up-regulation of cPLA2 and p-cPLA2. The E6+ transfects may have a growth advantage by its ability to migrate and formation of larger colonies compared to the E6- cells. Further studies are required to investigate whether the increased expression of cPLA2 and p-cPLA2 play a role in tumour genesis, invasion and migration of the E6+ cells when compared to E6-.

Both these isogenic cell lines are already cancer cells with altered mechanisms that give them growth advantages compared to normal cells, but it may also explain why the observed differences between them are not so great. Even so, our results suggest that additional alterations in cellular mechanisms as those attributed to the functions of the E6 viral protein, which targets p53 for degradation, seem to further enable cells into developing a more aggressive and invasive characteristic.

Although several interesting observations were made, the present study has some limitations. Firstly, we examined two time-points only and due to the slightly different growth rate of the cells, the stage of confluence was not reached at the same time. The confluent stage in the E6+ cells was closer to day five and thus the observed changes in cell size were much smaller than those of the E6- cells, which had reached confluence at Day 4. However, we did not want to confound results with the effects of apoptosis and necrosis that inevitably occur post-confluence, so time points for measuring metabolic alterations were therefore selected as Day 2 and Day 4. Secondly, we used only a single isogenic pair from a cell line that is not normally associated with HPV infection. However, because cervical cancer is almost always associated with HPV infection, the vast majority of cervical cancer cell lines available already contain this virus incorporated into the genome with expression of the E6 protein. Existing HPV-negative cervical cancer cell lines have other genetic transformations and altered metabolism compared with HPV-positive lines, hence a direct comparison between them would not account for non-HPV related genomic and metabolic modifications. In our isogenic model, the major difference was the presence of E6 protein making observed differences mainly ascribable to the effects of the E6 oncogene. In addition, these cells have previously been used in related studies as an acceptable model for the assessment of HPV-infection in cervical cancer [12, 14]. However, viral oncogenesis in the presence of the complete HPV genome would present much more complex effects on metabolism, as other HPV oncogenes, such as E7 and E5, would also be expressed and they are known to affect cellular proliferation and differentiation through diverse mechanisms [35].

Conclusion

Down-regulation of p53 rendered the E6+ cells somewhat slower in growth during a proliferative state than their empty vector counterparts with a corresponding reduction

in fatty acid and glucose metabolism. Cellular homeostasis was maintained through glutaminolysis. However, despite their reduced growth rate, the ability to migrate, form larger colonies and at slightly higher numbers given sufficient amount of time, suggests that the E6+ cells may have a growth advantage and perhaps be more invasive than un-transformed cells.

Acknowledgements

This work was partially funded by the Cancer Research UK and EPSRC Cancer Imaging Centre in association with MRC and Department of Health (England) grant no. C1060/A10334, NHS funding to the NIHR Biomedical Research Centre and the EC FP6 Marie Curie Action: Early Stage Training (contract No. 020718). We would also like to thank Dr MI Walton for the kind provision of the cell lines.

References

1 Bergler WF, Götte K: Current advances in the basic research and clinical management of juvenile-onset recurrent respiratory papillomatosis. Eur Arch Otorhinolaryngol 2000;257:263-269.
2 Mammas IN, Sourvinos G, Giannoudis A, Spandidos DA: Human papilloma virus (HPV) and host cellular interactions. Pathol Oncol Res 2008;14:345-354.
3 Huibregtse JM, Scheffner M, Howley PM: Localization of the E6-AP regions that direct human papillomavirus E6 binding, association with p53, and ubiquitination of associated proteins. Mol Cell Biol 1993;13:4918-4927.
4 Scheffner M, Huibregtse JM, Vierstra RD, Howley PM: The HPV-16 E6 and E6-AP complex functions as a ubiquitin-protein ligase in the ubiquitination of p53. Cell 1993;75:495-505.
5 Maddocks ODK ,Vousden KH: Metabolic regulation by p53. J Mol Med 2003;89:237-245.
6 Mahon MM, deSouza NM, Dina R, Soutter WP, McIndoe GA, Williams AD, Cox IJ: Preinvasive and invasive cervical cancer: an ex vivo proton magic angle spinning magnetic resonance spectroscopy study. NMR Biomed 2004;17:144–153.
7 Mahon MM, Williams AD, Soutter WP, Cox IJ, McIndoe GA, Coutts GA, Dina R, deSouza NM: 1H magnetic resonance spectroscopy of invasive cervical cancer: an in vivo study with ex vivo corroboration. NMR Biomed 2004;17:1-9.
8 Mountford CE, Delikatny EJ, Dyne M, Holmes KT, Mackinnon WB, Ford R, Hunter JC, Truskett ID, Russell P: Uterine cervical punch biopsy specimens can be analyzed by 1H MRS. Magn Reson Med 1990;13:324-331.
9 Delikatny EJ, Russell P, Hunter JC, Hancock R, Atkinson KH, van Haaften-Day C, Mountford CE: Proton MR and human cervical neoplasia: ex vivo spectroscopy allows distinction of invasive carcinoma of the cervix from carcinoma in situ and other preinvasive lesions. Radiology 1993;188:791-796.
10 Gottlieb E: P53 guards the metabolic pathway less travelled. Nat Cell Biology 2001;13:195-197.
11 Kawauchi K, Araki K, Tobiume K, Tanaka N: p53 regulates glucose metabolism through an IKK-NK- κB pathway and inhibits cell transformation. Nat Cell Biol 2008;10:611-618.
12 Vikhanskaya F, Vignati S, Beccaglia P, Ottoboni C, Russo P, D'Incalci M, Broggini M: Inactivation of p53 in a human ovarian cancer cell line increases the sensitivity to taxol by inducing G2 arrest and apoptosis. Exp Cell Res 1998;241:96–101.
13 Vikhanskaya F, Colella G, Valenti M, Parodi S, D'Incalci M, Broggini M: Cooperation between p53 and hMLH1 in a human colocarcinoma cell line in response to DNA damage. Clin Cancer Res 1999;5:937-941.
14 Vikhanskaya F, Falugi C, Valente P, Russo P: Human papillomavirus type 16 E6-enhanced susceptibility to apoptosis induced by TNF in A2780 human ovarian cancer cell line. Int J Cancer 2002;97:732–739.
15 Pestell KE, Hobbs SM, Titley JC, Kelland LR, Walton MI: Effect of p53 status on sensitivity to platinum complexes in a human ovarian cancer cell line. Mol Pharmacol 2000;57:503-511.
16 Tyagi RK, Azrad A, Degani H, Salomon Y: Simultaneous extraction of cellular lipids and water-soluble metabolites: evaluation by NMR spectroscopy. Magn Reson Med 1996;35:194-200.

17 Sitter B, Sonnewald U, Spraul M, Fjosne HE, Gribbestad IS: High-resolution magic angle spinning MRS of breast cancer tissue. NMR Biomed 2002;15:327-337.
18 Sze DY, Jardetzky O: Characterization of lipid composition in stimulated human lymphocytes by 1H-NMR. Biochim Biophys Acta 1990;1054:198-206.
19 Yasmeen A, Bismar TA, Kandouz M, Foulkes WD, Desprez PY, Al Moustafa AE: E6/E7 of HPV type 16 promotes cell invasion and metastasis of human breast cancer cells. Cell Cycle 2007;6:2038-2042.
20 Walboomers JM, Jacobs MV, Manos MM, Bosch FX, Kummer JA, Shah KV, Snijders PJ, Peto J, Meijer CJ, Muñoz N: Human papillomavirus is a necessary cause of invasive cervical cancer worldwide. J Pathol 1999;189:12-19.
21 Schwartzenberg-Bar-Yoseph F, Armoni M, Karnieli E: The tumour suppressor p53 down-regulates glucose transporter GLUT1 and GLUT4 gene expression. Cancer Res 2004;64:2627-2633.
22 Jiang P, Du W, Wang X, Mancuso A, Gao X, Wu M, Yang X: p53 regulates biosynthesis through direct inactivation of glucose-6-phosphate dehydrogenase. Nat Cell Biol 2011;13:310-316.
23 Boidot R, Végran F, Meulle A, Le Breton A, Dessy C, Sonveaux P, Lizard-Nacol S, Feron O: Regulation of monocarboxylate transporter MCT1 expression by p53 mediates inward and outward lactate fluxes in tumors. Cancer Res 2012;72:939-948.
24 Bonilla-Delgado J, Bulut G, Liu X, Cortés-Malagón EM, Schlegel R, Flores-Maldonado C, Contreras RG, Chung SH, Lambert PF, Uren A, Gariglio P: The E6 oncoprotein from HPV16 enhances the canonical Wnt/β-Caternin pathway in skin epidermis in vivo. Mol Cancer Res 2012;10:250-258.
25 Rampias T, Boutati E, Pectasides E, Sasaki C, Kountourakis P, Weinberger P, Psyrri A: Activation of Wnt signaling pathway by human papillomavirus E6 and E7 oncogenes in HPV16-positive oropharyngeal squamous carcinoma cells. Mol Cancer Res 2010;8:433-443.
26 Fragoso-Ontiveros V, María Alvarez-García R, Contreras-Paredes A, Vaca-Paniagua F, Alonso Herrera L, López-Camarillo C, Jacobo-Herrera N, Lizano-Soberón M, Pérez-Plasencia C: Gene expression profiles induced by E6 from non-European HPV18 variants reveals a differential activation on cellular processes driving to carcinogenesis. Virology 2012;432:81-90.
27 DeBerardinis RJ, Mancuso A, Daikhin E, Nissim I, Yudkoff M, Wehrli S, Thompson CB: Beyond aerobic glycolysis: transformed cells can engage in glutamine metabolism that exceeds the requirement for protein and nucleotide synthesis. Proc Natl Acad Sci USA 2007;104:19345-19350.
28 Gao P, Tchernyshyov I, Chang TC, Lee YS, Kita K, Ochi T, Zeller KI, De Marzo AM, Van Eyk JE, Mendell JT, Dang CV: c-Myc suppression of miR-23a/b enhances mitochondrial glutaminase expression and glutamine metabolism. Nature 2009;458:762-765.
29 Wise DR, DeBerardinis RJ, Mancuso A, Sayed N, Zhang XY, Pfeiffer HK, Nissim I, Daikhin E, Yudkoff M, McMahon SB, Thompson CB: Myc regulates a transcriptional program that stimulates mitochondrial glutaminolysis and leads to glutamine addiction. Proc Natl Acad Sci USA 2008;105:18782-18787.
30 Linkous A, Geng L, Lyshchik A, Hallahan DE, Yazlovitskaya EM: Cytosolic phospholipase A2, targeting cancer through the tumor vasculature. Clin Cancer Res 2009;15:1635–1644.
31 Yazlovitskaya EM, Linkous AG, Thotala DK, Cuneo KC, Hallahan DE: Cytosolic phospholipase A2 regulates viability of irradiated vascular endothelium. Cell Death Differ 2008;15:1641–1653.
32 Linkous AG, Yazlovitskaya EM, Hallahan DE: Cytosolic phospholipase A2 and lysophospholipids in tumor angiogenesis. J Natl Cancer Inst 2010;102:1398-1412.
33 MacPhail LB, Chung Y-L, Madhu B, Clark S, Griffiths JR, Kelland LR, Robinson SP: An investigation of tumour dose response to the vascular disrupting agent 5,6-dimethylxanthenone-4-acetic acid (DMXAA), using in vivo magnetic resonance spectroscopy. Clin Cancer Res 2005;11:3705-3713.
34 Chung Y-L, Troy H, Kristeleit R, Aherne W, Jackson LE, Atadja P, Griffiths JR, Judson IR, Workman P, Leach MO and Beloueche-Babari M: Non-invasive Magnetic Resonance Spectroscopic Pharmacodynamic Markers of a Novel Histone Deacetylase Inhibitor, LAQ824, in Human Colon Carcinoma Cells and Xenografts. Neoplasia 2008;10:303-313.
35 Liao S, Deng D, Hu X, Wang W, Li L, Li W, Zhou J, Xu G, Meng L, Wang S, Ma D: HPV16/18 E5, a promising candidate for cervical cancer vaccines, affects SCPs, cell proliferation and cell cycle, and forms a potential network with E6 and E7. Int J Mol Med 2013;31:120-128.